Article

Discovery Medicine 2024; 36(184): 1080–1090
https://doi.org/10.24976/Discov.Med.202436184.100

Needle-Free Injection of Metformin Ameliorates Skin Photoaging Through Inhibition of Ferroptosis and Oxidative Stress

Jingjing Zhang[1,2], Yonghong Qin[1], Jin Zhang[1], Xuanfen Zhang[1,*]

[1]Department of Plastic Surgery, Lanzhou University Second Hospital, 730030 Lanzhou, Gansu, China
[2]Department of General Surgery, Shanxi Provincial People's Hospital, 030012 Taiyuan, Shanxi, China
*Correspondence: zhang_xf@lzu.edu.cn (Xuanfen Zhang)
Published: 20 May 2024

Background: Skin photoaging is a complex process of skin aging caused by continuous exposure to ultraviolet (UV) radiation through oxidative stress and other pathways, yet effective treatments are scarce. Metformin is a drug with both anti-senescence and antioxidant functions; however, there are fewer studies on photoaging. The study aimed to investigate the role of needle-free injection of metformin in alleviating ultraviolet radiation B (UVB) induced skin photoaging, and to explore the mechanisms through which metformin alleviates fibroblast photoaging by inhibiting ferroptosis and oxidative stress.

Methods: In our study, we initially performed bioinformatic analysis on the gene expression profile (GSE38308), and our RNA sequencing (RNA-Seq) found that photoaging is associated with ferroptosis. We investigated the potential skin-protective mechanism of metformin by utilizing a UVB-induced rat skin photoaging model and human skin fibroblasts (HSF) treated with UVB. For *in vitro* experiments, cellular senescence was detected using SA-β-galactosidase staining and *p16* in western blot. Ferroptosis and oxidative stress were assessed via western blot (glutathione Peroxidase 4 (*GPX4*) and nuclear factor erythroid-2-related factor 2 (*Nrf2*)), reactive oxygen species (ROS) levels, transmission electron microscope, Lillie's staining, and immunofluorescence staining. During *in vivo* experiments, metformin was administered by needle-free jet injectors injected into the backs of rats. The effectiveness of metformin was detected using the Masson staining and western blot.

Results: We found that the ferroptosis pathway was closely associated with photoaging through bioinformatics analysis. In the UVB-induced photoaging HSF cells, treatment with metformin exhibits the following effects: a reduction in blue-stained granules in SA-β-galactosidase staining and a decrease in the expression of *p16*, indicating a reduction in cellular senescence. Moreover, metformin leads to decreased ROS levels and increased expression of the oxidative stress-related protein *Nrf2*, suggesting inhibition of oxidative stress within the cells. Additionally, metformin results in an elevation of *GPX4* expression, a decrease in blue-stained granules in Lillie's staining, and a reduction in ferroptosis-associated mitochondrial damage, indicating a decline in ferroptosis. Needle-free injection of metformin could directly achieve therapeutic effects by affecting HSF cells in the dermis. The needle-free injection of metformin treatment effectively improved the photoaging skin in rats compared to the photoaging group, ameliorated oxidative stress, and reduced ferroptosis.

Conclusions: Our data highlights a novel needle-free injection of metformin that improves photoaging and has good therapeutic potential.

Keywords: needle-free injection; photoaging; metformin; skin; ferroptosis

Introduction

Skin photoaging is a complicated process in which skin changes are caused by persistent ultraviolet (UV) exposure [1–3]. Epidemiological studies and surveys have shown that skin photoaging contributes to the development of numerous skin disorders and skin tumors [4,5]. Public health concerns regarding sun exposure on the skin have grown substantially in recent years as people recognize photoaging damages their health and beauty. Thus, preventing sun-induced skin photoaging is crucial.

UV radiation causes oxidative stress in the skin as the UV radiation interacts with skin tissues, causing an increase in reactive oxygen species (ROS) production [6–8]. Oxidative stress has been identified as a key factor in the pathogenesis of photoaging [3]. Imbalances in ROS production and removal result in ROS buildup and oxidative stress [9]. Oxidative stress and decreased cellular antioxidant levels are significant contributors to the development of ferroptosis [10,11]. Ferroptosis is a complex process that includes the buildup of iron ions, lipid peroxidation, interference with lipid synthesis pathways, disruption of the antioxidant defense system, and the participation of several regulatory

mechanisms. Additional study is required to comprehend the intricate regulatory mechanisms of these processes and to investigate therapeutic approaches for interfering in ferroptosis [10]. Previous research has shown that ferroptosis exists in photoaging skin, and antioxidants may decrease the incidence of ferroptosis [12,13]. Metformin effectively treats various diseases by reducing inflammation, oxidative stress, and DNA damage [14,15]. Although metformin is increasingly used to treat skin diseases, whether it alleviates skin UV damage by inhibiting ferroptosis is still unclear [16,17].

Photoaging of the skin is a condition of extrinsic aging caused by prolonged exposure to UV radiation [18]. Cellular senescence is a complex biological process involving normal cells ceasing to divide and experiencing functional decline for various reasons [19]. Skin aging is a manifestation of cellular senescence at the level of the skin organ and is closely related to cellular senescence [19–21]. In our research, we investigated the treatment of skin photoaging at the level of fibroblast aging. Presently, the efficacy of medications like creams, which are used to mitigate and prevent skin photoaging, is constrained by their inadequate dermal penetration [22]. Needle-free injectors, renowned for their safety and effectiveness, have been extensively used for local anesthetic and vaccination delivery, especially for those who suffer from needle phobia [23,24]. Needle-free jet injectors efficiently administer the whole medication into the skin's dermis, explicitly targeting and improving the aging condition of fibroblasts in that area.

In this study, our transcriptome sequencing data of human skin fibroblasts (HSF) photoaging mode was compared to data of GSE38308 in GEO; we identified the most critical ferroptosis genes for photoaging. We injected metformin into the back skin of photoaging rats using needle-free jet injectors to address the issue of inadequate medication penetration. We determined the role of metformin in ameliorating ferroptosis and preventing skin photoaging.

Methods

Bioinformatic Analysis

We selected the GSE38308 expression profiling dataset, which was downloaded from the Gene Expression Omnibus (GEO) database (https://www.ncbi.nlm.nih.gov/geo/query/acc.cgi?acc=GSE38308). The dataset includes 21 pairs of sun-exposed pre-auricular and sun-protected post-auricular skin samples from northern Chinese women. To screen suitable samples for finding the potential functional biomarkers or therapeutic targets, we used weighted gene co-expression network analysis (WGCNA) to analyze the genes in the skin tissues of patients with photoaging. This analysis was performed using the R package (WGCNA, version 1.71, University of California, Los Angeles, CA, USA) in the R software (version 4.1.0, R Project for Statistical Computing, Vienna, Austria; https://www.r-project.org/). The first step was to cluster samples and then check whether they contained outliers due to human or other reasons. These outlier samples would affect the subsequent results. To minimize these issues, in a second step, samples that did not belong to the same network topology were deleted (**Supplementary Fig. 1**). We also selected the transcriptome RNA sequencing (RNA-Seq) data for the photoaging HSF cell. Our RNA-Seq data were the high-throughput sequencing by using an Illumina Hiseq sequencing platform (https://dataview.ncbi.nlm.nih.gov/object/PRJNA1036444?reviewer=fuhdtjeaaprom2td9p6qa70933). The ferroptosis-related gene sets were extracted from FerrDb (http://www.zhounan.org/ferrdb/) and KEGG (https://www.kegg.jp/). Using the limma package, we screened for significantly different expression genes (DEGs). An adjusted false discovery rate $p < 0.01$ and |log2 fold change (FC)| >0.585 were set as the threshold for identifying significant DEGs. The ferroptosis genes related to photoaging were identified using bioinformatics analysis.

HSF Cells Culture and Treatment

Immortalized human skin fibroblasts (HSF cells) were obtained from iCell Bioscience Inc (#iCell-0051a, Shanghai, China). Following the examination, it was determined that there was no presence of mycoplasma contamination in the HSF cells. Additionally, the short tandem repeats (STR) identification confirmed that the cells were really fibroblasts. The HSF cells were cultured in DMEM/F12 medium (#11330057, Gibco, Los Angeles, CA, USA) supplemented with 10% fetal bovine serum (#FSP500, ExCell Bio, Suzhou, China). Culturing was conducted in an incubator at 37 °C with 5% CO_2. Utilizing the CCK-8 kit (#M4839, Abmole, Houston, TX, USA) and optical density measurement at 450 nm, cell viability was ascertained to assess and ascertain the suitable dosage of metformin (MF, #M3244, Abmole, Houston, TX, USA) and ultraviolet radiation B (UVB). Following our experimentation, the application of 100 µM metformin has been shown to dramatically enhance the viability of HSF cells when exposed to 20 mJ/cm^2 UVB irradiation. Thus, 100 µM was determined as the following metformin concentration of cell and needle-free injection.

Transcriptome RNA Sequencing

HSF cell from the control and photoaging groups (n = 3) was prepared as described for standardized sample processing and was sent to the Novogene Biotechnology Co., Ltd. (Tianjin, China) for high-throughput sequencing using an Illumina Hiseq sequencing platform. RNA integrity was assessed using the RNA Nano 6000 Assay Kit (#G2938-80023, Agilent Technologies, Los Angeles, CA, USA) of the Bioanalyzer 2100 system (Agilent Technologies, Los Angeles, CA, USA). Total RNA was used as the starting material for the RNA sample preparations. To sum-

marize, mRNA was isolated from total RNA using poly-Toligo-attached magnetic beads. Then, synthesize double-stranded cDNA. The library fragments were purified using the AMPure XP (#AA63882, Beckman Coulter, Los Angeles, CA, USA) technology to select cDNA fragments ranging from 370 to 420 bp. The PCR was then carried out using Phusion High-Fidelity DNA Polymerase, Universal PCR primers, and Index (X) Primer. Finally, PCR products were purified, and library quality was tested using the Bioanalyzer 2100 system (Agilent Technologies, Los Angeles, CA, USA). The pretreated data were subjected to quality control by FastQC software (version 0.12.1, Babraham Institute, Cambridge, Cambridgeshire, UK) and then analyzed for DEGs. If the $|\log2 \text{ fold change (FC)}| > 0.585$ and the adjusted p-value was <0.05, the gene was considered differentially expressed.

Rats Culture and Treatment

The 18 male SPF-grade SD rats aged 6 weeks and weighing 120–150 g, were obtained from the experimental animal center at Lanzhou University. The rats were housed per cage in the SPF-grade environment with a 12-hour light-dark cycle and free access to food and water. 18 male rats were randomly divided into the following groups (3 rats per group): the transdermal injection group and the needle-free injection group, the control group, UVB group, UVB+metformin (MF) group, and UVB+RA (0.025% Retinoic acid cream, #H50021817, Huabang Pharm, Chongqing, China) group. The *in vivo* experimental techniques were authorized by the Committee in the Use of Animals of Lanzhou University Second Hospital (No. D2022-294), and all operations involving animals were performed following the Guide for the Care and Use of Laboratory Animals.

Rats Treatment

To compare the damage to the dermis between the transdermal injection and the needle-free injection.

In the transdermal injection group, the back skin of 3 rats was injected once every 2 days for 15 days using the regular injector. The injection volume for each site is 0.2 mL PBS, with a total of 15 different sites.

In the needle-free injection group, the back skin of 3 rats was injected once every 2 days for 15 days using the needle-free injector. The injection volume for each site is 20 µL PBS, comprising 15 different sites. Needle-free jet injectors (#ZHT-A, Zhonghuishengxi Inc, Qingdao, China) efficiently administer the whole medication into the skin's dermis.

We used the following intervention measures to compare the effectiveness of needle-free injection of metformin in improving skin photoaging.

In the control group, 3 rats were housed in the SPF-grade environment without UVB irradiation.

In the photoaging group (UVB group), the back skin of 3 rats was irradiated with UVB radiation. The rats were irradiated dorsally using the UVB lamps (30 W, 2 tubes, irradiance 290–320 nm, #TL-30 RS UVB, Philips, Amsterdam, Netherlands) five times a week for 8 weeks. The energy of UVB irradiation was progressively increased from 60 mJ/cm^2 in the first week to 120 mJ/cm^2, 180 mJ/cm^2, and 240 mJ/cm^2 through the final weeks [25,26]. The total UVB dose was approximately 7.8 J/cm^2. Irradiation intensity was measured using a UVB meter (#WXS10, Handy, Beijing, China).

In the UVB+MF group, 20 µL 100 µM MF by needle-free jet injectors was injected into the back skin of 3 rats simultaneously with the beginning time of UVB irradiation. Needle-free jet metformin delivery consisted of one-time injections in 15 different sites evenly on the whole dorsal skin.

In the UVB+RA group, the 3 photoaging rats were daubed 0.025% Retinoic acid cream on the back as a positive control group. The 0.025% Retinoic acid cream was the most potent treatment option for photoaging [27,28].

Each rat's whole back skin was divided into at least three parts to be analyzed. After 8 weeks of intervention, the rats were euthanized rats by excessive anesthesia with pentobarbital overdose (dosage: 150 mg/kg) [29]. The skin tissues were then obtained, and then conducted in subsequent experiments.

Western Blot

The protein of HSF and rat skin tissue were extracted using RIPA (#P0013B, Beyotime Technologies, Shanghai, China). The proteins were separated by SDS-PAGE and transferred to PVDF membranes (0.22 µm, #PR05507, Millipore Inc, Billerica, MA, USA). The membranes were blocked with 5% BSA and incubated overnight at 4 °C with the following primary antibodies (purchased from Affinity Biosciences, Liyang, China): glutathione Peroxidase 4 (*GPX4*) (#DF6701; 1:1000), *p16* (#AF5484; 1:1000), nuclear factor erythroid-2-related factor 2 (*Nrf2*) (#AF0639; 1:1000), and β-actin (#AF7018; 1:1000). The photoaging model was estimated by using western blot of senescence-associated protein levels of *p16* [30–32]. The antioxidant status was estimated by using western blot and of *Nrf2*. After being incubated with HRP (horseradish peroxidase)-conjugated anti-rabbit IgG (H+L) antibody (#S0001; 1:1000; Affinity Biosciences, Liyang, China) coupled to horseradish peroxidase. Electrochemical luminescence (ECL, #BL520B, Biosharp, Guangzhou, China) reagent was used for immune detection and visualization using a Fully automatic chemiluminescence image processing system (Tanon 5200 Multi, Tanon, Shanghai, China). The β-actin was used as a control. The quantitative analysis of protein bands was performed using ImageJ software (Version2020, National Institutes of Health, Bethesda, MD, USA).

Staining Examination

SA-β-galactosidase activity was determined for HSF cells using the Senescent β-galactosidase staining kit (#G1580, Solarbio Science & Technology, Beijing, China). The cells were then fixed with 10% formalin (pH 7.4) at room temperature for 15 min. Next, the cells were incubated in freshly prepared β-galactosidase staining solution at 37 °C free of CO_2 incubator overnight. The quantitative analysis of protein bands was performed using ImageJ software (Version 2020, National Institutes of Health, Bethesda, MD, USA).

After being immersed in 4% paraformaldehyde for 48 hours, the skin tissues of the rats were allowed to dry out; then, they were embedded in paraffin and sliced into 4 µm sections. The aging histological situation of the rat photoaging model was determined by the hematoxylin-eosin (H&E) staining kit (#G1120, Solarbio Science & Technology, Beijing, China). The Masson staining kit (#G1343, Solarbio Science & Technology, Beijing, China) was utilized to identify the change of collagen fibers with photoaging. The histological alterations of the skin were observed under a microscope (BX53+DP74, Olympus, Tokyo, Japan).

Immunofluorescence

Immunofluorescence staining was used to observe the expression of the target protein in the photoaging HSF and rat skin. The pre-treatment for incubating primary antibodies is as follows: (1) HSF was transparent in 0.2% Triton X-100 (T8200, Solarbio Science & Technology, Beijing, China). (2) Each group's paraffin sections (4 µm) were dewaxed, hydrated, and antigen repaired. 5% bovine serum albumin (BSA, #SW3015, Solarbio Science & Technology, Beijing, China) was used to block non-specific binding for 1 h. After blocking, the samples were treated with primary antibodies (*GPX4* and *Nrf2*, 1:500, same as the primary antibody in WB) at 4 °C overnight. The following day, the samples were treated with secondary antibodies at 4 °C for 1 h. The secondary antibodies were purchased from Affinity Biosciences (Liyang, China): Goat anti-Rabbit IgG (H+L) FITC-conjugated (#S0008; 1:2000) and Goat anti-Rabbit IgG (H+L) CY3-conjugated (#S0011; 1:2000). The samples were mounted using the antifade mounting medium with DAPI (#S2110, Solarbio Science & Technology, Beijing, China). The immunofluorescence staining histological alterations of the skin were observed under a microscope (BX53+DP74, Olympus, Tokyo, Japan).

Transmission Electron Microscope (TEM)

Following an overnight fixation in 10% glutaraldehyde, cell samples were treated with 1% osmic acid. A succession of ethanol and acetone was used to rehydrate the samples after they were washed with PBS. After that, ultrathin slides were created on the ultramicrotome and then submerged and embedded in ethoxylate resin. The cell samples were observed via transmission electron microscopy (#HT7800, HITACHI Inc, Tokyo, Japan) after double-staining the slides with uranyl acetate and lead citrate.

Detection of Intracellular ROS

ROS test kits (#50101ES01, Yeasen Biotechnology, Shanghai, China) were used to analyze average ROS levels following the manufacturer's protocol. The HSF cells were washed with PBS, and a medium containing 10 µM 2′,7′ Dichlorodihydrofluorescein diacetate (DCFH-DA) was added for co-incubation at 37 °C for 20 minutes. Subsequently, the fluorescently labeled cells were washed twice with PBS and measured using a flow cytometry (CytoFLEX S, Beckman Coulter, CA, USA) within 30 min.

Statistical Analysis

The results were analyzed using SPSS 25.0 (IBM Corp., Armonk, NY, USA). The overall significance of the data was assessed using a one-way analysis of variance with the Bonferroni adjustment for group comparisons. A p-value of <0.05 was considered statistically significant. Image Pro Plus 6.0 (Media Cybernetics Inc, Rockville, MD, USA) was used to assess positively stained regions in this investigation.

Results

Identification of Ferroptosis-Related DEGs in Photoaging Skin

The WGCNA analysis of GSE38308 showed the clustering of 21 groups (42 samples) of skin samples from patients with and without skin photoaging, with 12 outlier non-cluster samples (**Supplementary Fig. 1**). Thus, after removing these outlier samples, other samples (including 14 photoaging samples and 16 healthy normal samples) were used for further analysis. The R software (version 4.1.0, R Project for Statistical Computing, Vienna, Austria; https://www.r-project.org/) was used to filter ferroptosis-related DEGs in GSE38308 and our RNA-Seq data. After normalization, 43 ferroptosis-related DEGs were identified in photoaging samples compared to control samples in GSE38038 (Fig. 1A). 29 ferroptosis-related DEGs were identified in our RNA-Seq data (Fig. 1B). The intersection of ferroptosis genes identified from the above two datasets resulted in four common genes (Fig. 1C). These 4 genes were *ATF3* (activating transcription factor 3), *GOT1* (glutamic-oxaloacetic transaminase 1), *GPX4*, and *PRDX6* (peroxiredoxin 6). The relative expression levels of 4 genes are shown in Fig. 1D,E. These findings suggest the potential involvement of ferroptosis in skin photoaging. Notably, GPX4 was selected for in-depth investigation due to its pivotal role in the ferroptosis pathway.

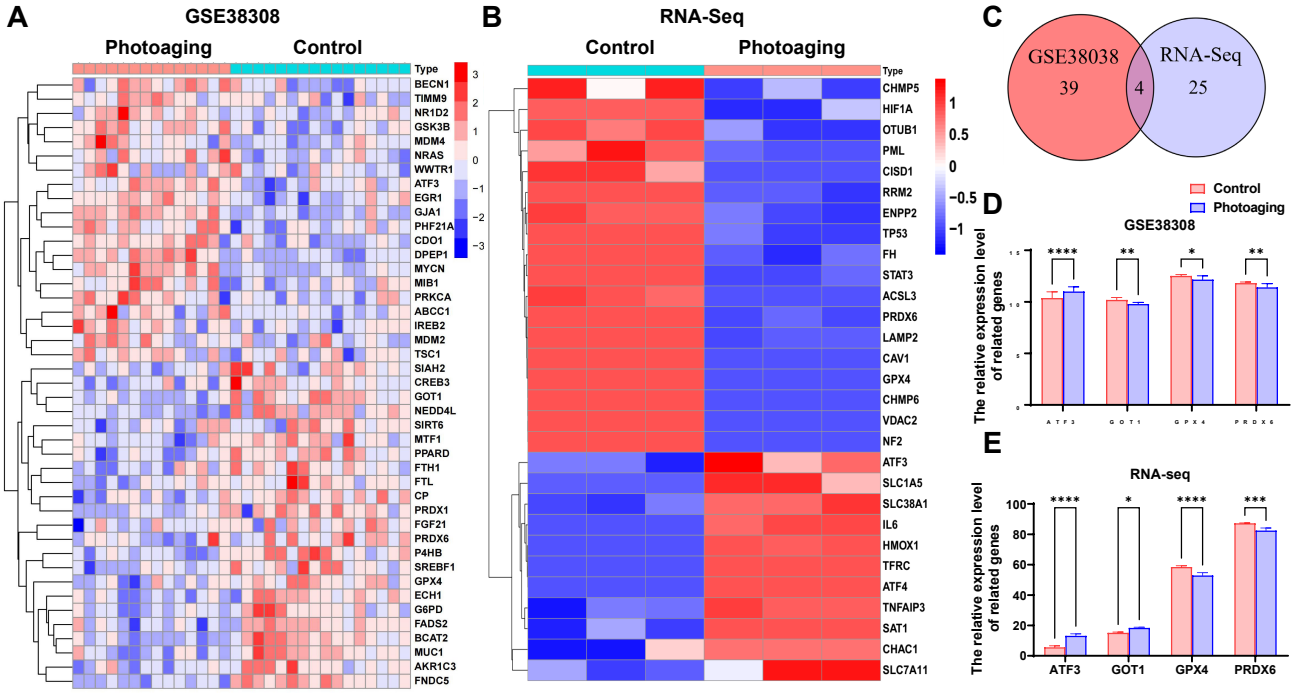

Fig. 1. Identification of ferroptosis-related different expression genes (DEGs) in photoaging skin. (A) The ferroptosis-related DEGs of the GSE38308 dataset. (B) The ferroptosis-related DEGs of our RNA-Seq dataset. (C) The Venn gram of ferroptosis-related DEGs in 2 datasets. (D,E) The relative expression levels of intersecting genes in two datasets. 6 samples were tested in each group, and the experiment was repeated 3 times. * $p < 0.05$, ** $p < 0.01$, *** $p < 0.001$, **** $p < 0.0001$. RNA-Seq, RNA sequencing; *GPX4*, glutathione Peroxidase 4; *ATF3*, activating transcription factor 3; *GOT1*, glutamic-oxaloacetic transaminase 1; *PRDX6*, peroxiredoxin 6.

Metformin Could Ameliorate Photoaging HSF Cells

In the present study, we first confirmed and investigated that metformin could ameliorate the photoaging effects of 20 mJ/cm^2 UVB irradiation on HSF cells. The UVB-irradiated group had a significantly higher percentage of SA-β-galactosidase-stained HSF cells than the control group (Fig. 2A,G). After UVB irradiation, HSF cells expressed *p16* much more than the control group (Fig. 2B). According to our findings, UVB may cause HSF cell photoaging. We used metformin for intervention and found that metformin promotes the vitality of photoaging HSF cells in a dose-dependent manner. The survival rates of photoaging HSF cells with 100 µM metformin and UVB (20 mJ/cm^2) were the highest. Compared to photoaging cells, the UVB+metformin group (UVB+MF) showed fewer blue particles of SA-β-galactosidase staining (Fig. 2A,G). Compared with the UVB group, the *p16* protein expression level was significantly downregulated in the UVB+MF group (Fig. 2B,I). Thus, the results indicated that metformin can effectively improve photoaging.

Metformin Could Attenuate Oxidative Stress and Ferroptosis in Photoaging HSF Cells

UVB exposure leads to increased oxidative stress in HSF cells. *Nrf2* is a central transcription factor regulating antioxidant responses [33,34]. The increase in elevation of *Nrf2* signifies an enhancement in the capacity to withstand oxidative stress damage [35]. In flow cytometry analysis, the UVB group had higher ROS levels and lower *Nrf2* protein expression than the control group (Fig. 2B,C,H,I). Compared to the UVB group, the UVB+MF group could decrease oxidative stress and enhance *Nrf2* protein expression (Fig. 2B,C,H,I).

The Lillie's staining exhibited blue particles, suggesting Fe^{2+} buildup in the UVB group (Fig. 2D). Our investigation also found ferroptosis in UVB-treated HSF cells. TEM showed higher mitochondrial membrane density and wrinkling (Fig. 2E). In the UVB+MF group, the occurrence of ferroptosis was reduced, and the protein expression of *GPX4* was higher than in the UVB group (Fig. 2F). The results showed that metformin can ameliorate oxidative stress and ferroptosis. Thus, metformin is a potential drug to investigate a possible strategy to prevent skin aging.

Effectiveness of Metformin Delivery with a Needle-Free Injector

To effectively control photoaging, metformin must reach the dermis, which is located underneath the skin's outermost layer. A transdermal injection of a concentrated dose of metformin caused accumulation. Fig. 3A shows that the needle-free injector caused less skin injury than transdermal injection. More subcutaneous bubbles appear at transdermal injection sites, which may be due to partial

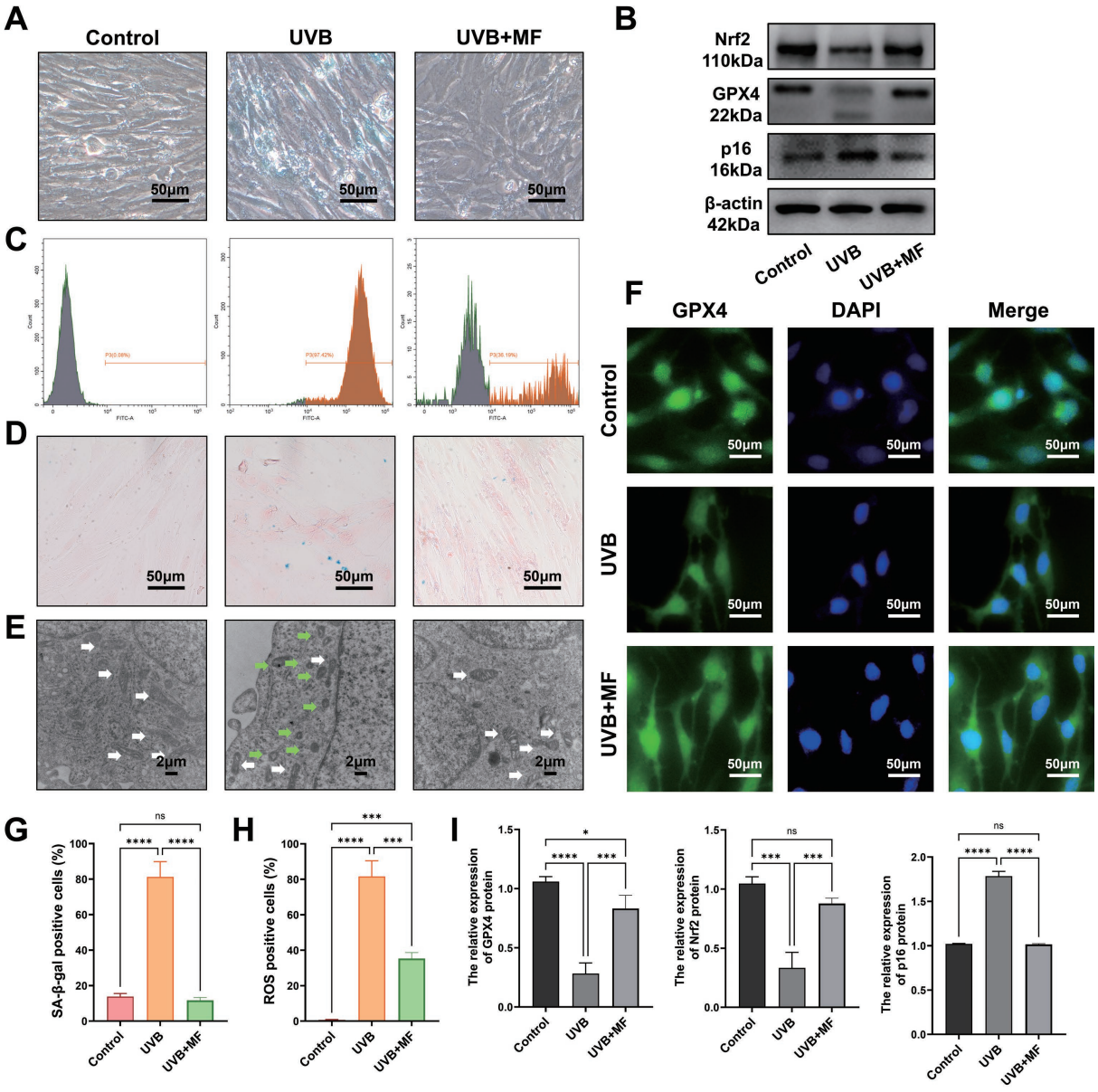

Fig. 2. Metformin ameliorates photoaging human skin fibroblasts (HSF) cells by inhibiting ferroptosis. (A) The SA-β-galactosidase staining in control, photoaging, and ultraviolet radiation B (UVB)+metformin (MF) groups. (B) The *p16*, *GPX4*, and nuclear factor erythroid-2-related factor 2 (*Nrf2*) in each group were determined by western blot. (C) The reactive oxygen species (ROS) was evaluated by performing flow cytometry for each group. (D) The Lillie staining each group (the presence of blue particles represented Fe^{2+} accumulation). (E) Transmission electron microscope (TEM) of mitochondria in cell samples in each group (magnification, $\times$10,000), the white arrows represent normal mitochondria, and the green arrows represent abnormal mitochondria. (F) The immunofluorescence of *GPX4* in each group. (G) The SA-β-galactosidase staining positive cells (%) in each group. (H) ROS positive cells (%) in each group. (I) The ratio of *GPX4*, *Nrf2*, *p16*/β-actin each group. 6 samples were tested in each group, and the experiment was repeated 3 times. ns $p > 0.05$, * $p < 0.05$, *** $p < 0.001$, **** $p < 0.0001$.

cellular necrosis. On the other hand, there is no obvious harm from needle-free injections (Fig. 3B). The findings showed that deep skin tissue interventions may be accomplished with minimum injury using needle-free injections.

The Needle-Free Injection of Metformin Exerted Anti-Ferroptosis and Anti-Oxidative Stress Effects to Protect the Skin

In a UVB-induced skin-photoaging rat model, we evaluated the efficacy of needle-free injection in metformin-driven amelioration of skin aging. As shown

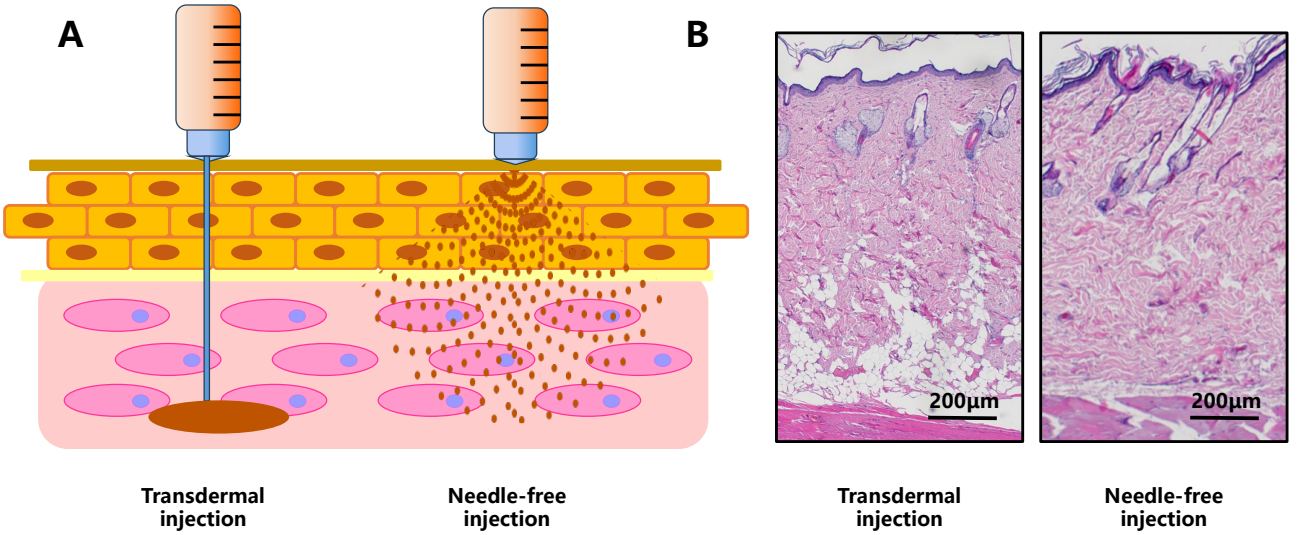

Fig. 3. Effectiveness of metformin delivery with a needle-free injector. (A) Schematic illustration of transdermal injection and needle-free injection (drawn by powerpoint software (version 2021, Microsoft, Los Angeles, CA, USA)). (B) Hematoxylin-eosin (H&E) staining of representative skin histology in each group. 6 samples were tested in each group, and the experiment was repeated 3 times.

in Fig. 4A, the control group had essentially no signs of wrinkles. On the other hand, the UVB group develops deep and broad wrinkles due to UVB exposure. Wrinkles in the groups with needle-free metformin injection therapy were less deep and thinner. Even after the same amount of time under UVB treatment, deep wrinkles were still visible in the UVB+RA group treated with 0.025% Retinoic acid cream, as opposed to the UVB+MF group. Histology of the skin revealed metformin affected the quantity of collagen deposited and the structural alterations in the dermal layer. Masson's Trichrome staining revealed alterations in dermal collagen content. Collagen fibers were seen in a consistent arrangement in the control group. The UVB group had more aberrant, fractured, and disordered collagen fibers due to UV irradiation than the control group. All treated groups showed improvements in UV-induced damage to collagen fibers, but the improvement effect of the UVB+MF group was more significant than that of the UVB+RA group (Fig. 4B). In addition, we verified the protein level of skin samples in each group to observe whether needle-free injection of metformin can effectively alleviate the occurrence of aging, oxidative stress, and iron death in photoaging skin. We analyzed *p16*, *Nrf2*, and *GPX4* using western blot (Fig. 4C,D). Compared with the UVB group, the western blot and immunofluorescence results showed that needle-free injection of metformin exerted anti-ferroptosis and anti-oxidative stress effects to protect the skin (Fig. 4C,E). Under the same duration, the improvement effect of the UVB+RA group was limited. In general, needle-free injection of metformin was the most effective in protecting skin from photoaging, and the effect was better than that of 0.025% Retinoic acid cream.

Discussion

Sunlight and other forms of exogenous skin damage pose serious health risks. Solar UVA (ultraviolet radiation A) and UVB rays account for most of the sun's ultraviolet radiation. Because it may enter the dermis, ultraviolet B can harm elastin and collagen. Light from the sun causes photoaging, sunburn, pigmentation, and even skin cancer by inducing a cascade of molecular changes, including inflammation, DNA and protein damage, and ROS generation. Mitochondrial damage, impaired cellular material production, impaired metabolic activity, and, ultimately, cell death may all be caused by ROS [8]. This is one of the many steps leading to abnormal iron metabolism and, eventually, the triggering of ferroptosis is an increased ROS in cells.

Based on the bioinformatics analysis of our RNA-Seq dataset and the GSE38308, ferroptosis might be a phenomenon in photoaging skin. We identified genes linked to the ferroptosis deficit by collecting differential genes and conducted studies on those genes. Under UVB irradiation, skin fibroblasts produce most ROS. *GPX4* stops peroxides on membrane lipids and protects cell membranes by converting glutathione (GSH) to its oxidized form (GSSG). When the cellular antioxidant system metabolism is abnormal, GSH is depleted, and *GPX4* activity decreases, inhibiting lipid peroxide processing via the glutathione reduction route, as previously demonstrated [12].

Current therapies mainly focus on senescence, antioxidation, free radical scavenging, and other strategies to activate the endogenous adaptive defenses. Metformin is a drug that has both anti-senescence and antioxidant functions. First, we conducted experiments on metformin in a photoaging model of HSF cells. Metformin also reversed the increase in ferroptosis in mitochondria and oxidative stress

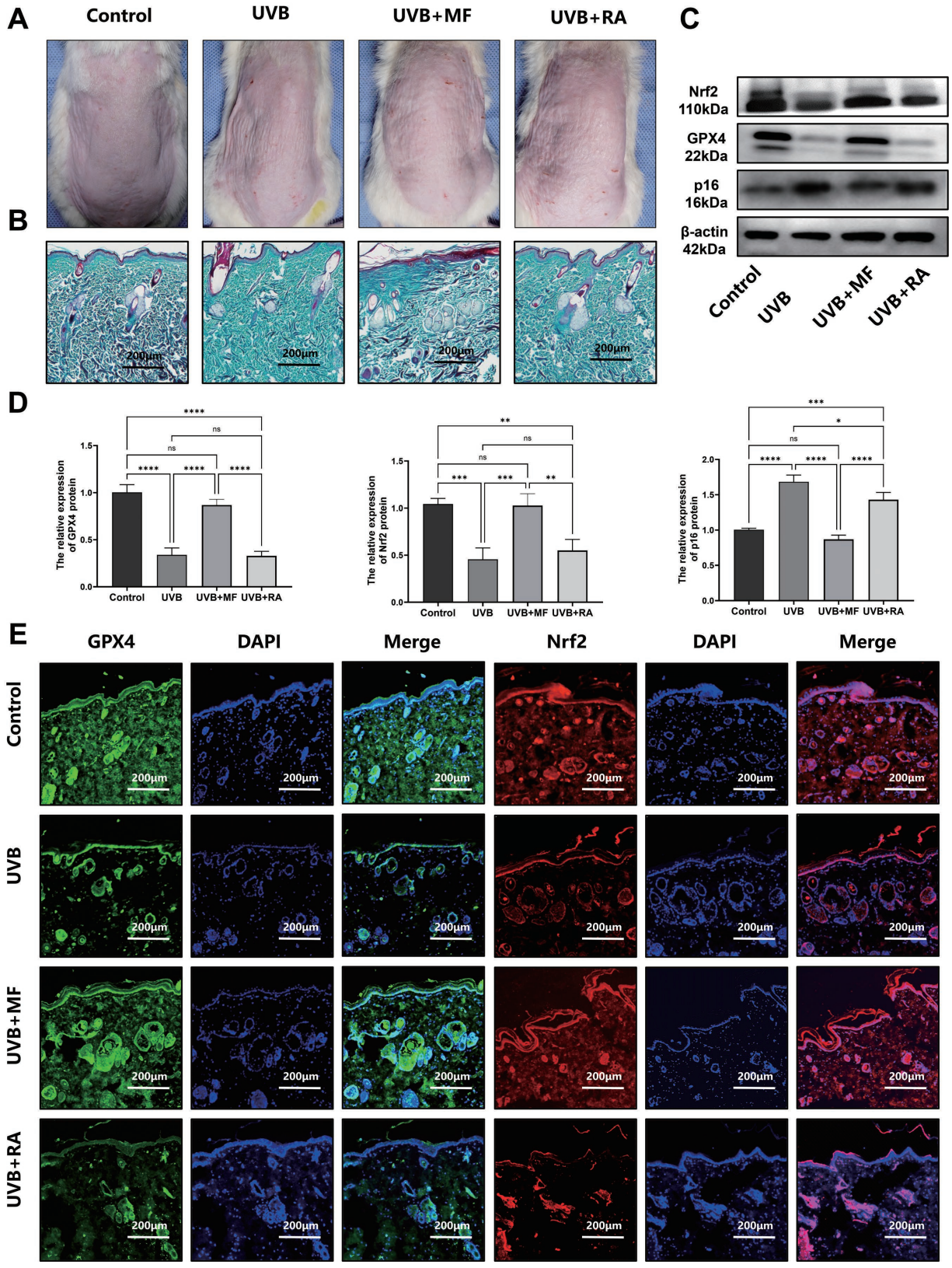

Fig. 4. The needle-free injection of metformin exerted anti-ferroptosis and anti-oxidative stress effects to protect the skin. (A) Photographs of dorsal skin of mice from different groups. (B) Masson staining of skins in each group. (C,D) The *p16*, *GPX4*, and *Nrf2* of each group were determined by western blot. (E) *GPX4* and *Nrf2* in the skin of different groups determined by immunofluorescence. 6 samples were tested in each group, and the experiment was repeated 3 times. ns $p > 0.05$, * $p < 0.05$, ** $p < 0.01$, *** $p < 0.001$, **** $p < 0.0001$. RA, Retinoic acid.

induced by UVB. The preliminary verification also showed that metformin promoted *Nrf2* expression and increased the expression of *GPX4*, inhibiting ferroptosis. *Nrf2* is a key transcription factor that plays a critical role in combating UV-induced skin damage. Activation of *Nrf2* promotes the expression of downstream antioxidant response genes such as *HO-1* (Heme Oxygenase 1), directly or indirectly enhancing cellular antioxidant capacity, reducing oxidative stress and cellular toxicity caused by ROS, thereby protecting the skin from UV radiation damage [36–38]. Additionally, research has found that *Nrf2* activation can reduce the expression of matrix metalloproteinase-1 (MMP-1) induced by UV, inhibiting collagen degradation and slowing skin aging [39]. Furthermore, *Nrf2* is also a driver gene that inhibits ferroptosis, and its activation can regulate ferroptosis through HO-1 [40]. Metformin can alleviate oxidative stress in endothelial cells by activating AMPK (AMP-activated Protein Kinase) [41]. The role of AMPK in anti-aging mainly involves its regulation of cellular energy balance and metabolic state [42]. AMPK, a highly conserved energy sensor, is activated when intracellular ATP levels decrease, maintaining the balance of ATP generation and consumption in eukaryotic cells, namely energy homeostasis [43]. This process is of great significance for delaying aging and extending lifespan. Studies have shown that loss of AMPK reduces DNA repair in UVB-induced skin cells, while the activator of AMPK, metformin, enhances DNA repair and prevents photoaging in skin cells [44–47]. UVA irradiation can cause DNA double-strand breaks and DNA base damage and inhibit DNA repair, leading to cell apoptosis and skin cell aging [48]. UV irradiation activates the *PI3K/AKT/mTOR* (Phosphoinositide 3-Kinase/Protein Kinase B/mammalian Target of Rapamycin) signaling pathway's self-repair and renewal capabilities, preventing cell apoptosis, maintaining cell survival, and accelerating DNA repair [49]. However, long-term UV exposure may excessively activate the *PI3K/AKT/mTOR* signaling pathway, leading to DNA damage repair failure and cell tumorigenesis [49,50]. In this case, metformin reduces DNA damage by reducing cellular oxidative stress, inhibiting excessive activation of the *PI3K/AKT/mTOR* signaling pathway, maintaining it at normal levels, and preventing skin cell carcinogenesis [51].

For efficient regulation of photoaging skin tissue, metformin has to penetrate the skin's outermost layer to access the dermis. Inadequate penetration into the deep dermis limits the efficacy of topical cream treatments despite their widespread usage to address skin aging. Nodules and localized tissue injury may occur at the injection site when syringes are used for transdermal injections. Thanks to its reusable design, lack of needle phobia, and the absence of needle stick injuries, needle-free injection technology has substantially enhanced long-term insulin injection and mass immunization programs. A commercially available jet injector is a needle-free device that propels exosome solution into the dermis of the skin using pneumatic force. Herein, we evaluated its performance to reduce the effects of photoaging, oxidative stress, and ferroptosis with a needle-free injection of metformin. Compared with Retinoic acid cream, the findings demonstrated that needle-free injection of metformin provided superior photoaging protection for the skin.

Conclusions

In conclusion, we showed that ferroptosis plays a role in photoaging. By suppressing oxidative stress and ferroptosis, metformin can ameliorate photoaging. The application of metformin via needle-free injection, which targets dermal cells directly, proves to be more efficacious in decelerating skin aging compared to the conventional application of Retinoic acid cream.

Availability of Data and Materials

The datasets (GSE38308) presented in this study can be found in the online GEO database: https://www.ncbi.nlm.nih.gov/geo/query/acc.cgi?acc=GSE38308. Our transcriptome RNA sequencing data is currently being uploaded to the GEO database: https://dataview.ncbi.nlm.nih.gov/object/PRJNA1036444?reviewer=fuhdtjeaaprom2td9p6qa70933.

Author Contributions

Conceptualization, YHQ and JJZ; methodology, JJZ; software, YHQ; validation, JJZ and JZ; formal analysis, JJZ; investigation, JJZ; resources, JJZ; data curation, XFZ; writing—original draft preparation, JJZ; writing—review and editing, XFZ; visualization, JZ; supervision, XFZ; project administration, XFZ; funding acquisition, YHQ. All authors contributed significantly to editorial changes of important content. All authors have read and agreed to the published version of the manuscript. All authors provided feedback on earlier drafts of the paper. The final text was reviewed and approved by all authors.

Ethics Approval and Consent to Participate

The *in vivo* experimental techniques were authorized by the Committee in the Use of Animals of Lanzhou University Second Hospital (No.D2022-294), and all operations involving animals were performed following the Guide for the Care and Use of Laboratory Animals.

Acknowledgment

Not applicable.

Funding

This work was funded by the Cuiying Scientific and Technological Innovation Program of Lanzhou University Second Hospital (Grant No.CY2022-MS-A13).

Conflict of Interest

The authors declare no conflict of interest.

Supplementary Material

Supplementary material associated with this article can be found, in the online version, at https://doi.org/10.24976/Discov.Med.202436184.100.

References

[1] Zhu S, Zhao Z, Qin W, Liu T, Yang Y, Wang Z, *et al*. The Nanostructured lipid carrier gel of Oroxylin A reduced UV-induced skin oxidative stress damage. Colloids and Surfaces. B, Biointerfaces. 2022; 216: 112578.

[2] Prokopov A, Drobintseva A, Kvetnoy I, Gazitaeva Z, Sidorina A. Effect of a hyaluronic acid-based mesotherapeutic injectable on the gene expression of CLOCK and Klotho proteins, and environmentally induced oxidative stress in human skin cells. Journal of Cosmetic Dermatology. 2023; 22: 156–172.

[3] Chen X, Yang C, Jiang G. Research progress on skin photoaging and oxidative stress. Postepy Dermatologii i Alergologii. 2021; 38: 931–936.

[4] Termer M, Jaeger A, Carola C, Salazar A, Keck CM, Kolmar H, *et al*. Methoxy-Monobenzoylmethane Protects Skin from UV-Induced Damages in a Randomized, Placebo Controlled, Double-Blinded Human In Vivo Study and Prevents Signs of Inflammation While Improving the Skin Barrier. Dermatology and Therapy. 2022; 12: 435–449.

[5] Zhong QY, Lin B, Chen YT, Huang YP, Feng WP, Wu Y, *et al*. Gender differences in UV-induced skin inflammation, skin carcinogenesis and systemic damage. Environmental Toxicology and Pharmacology. 2021; 81: 103512.

[6] Mokrzyński K, Krzysztyńska-Kuleta O, Zawrotniak M, Sarna M, Sarna T. Fine Particulate Matter-Induced Oxidative Stress Mediated by UVA-Visible Light Leads to Keratinocyte Damage. International Journal of Molecular Sciences. 2021; 22: 10645.

[7] Krutmann J, Schalka S, Watson REB, Wei L, Morita A. Daily photoprotection to prevent photoaging. Photodermatology, Photoimmunology & Photomedicine. 2021; 37: 482–489.

[8] Tan CYR, Tan CL, Chin T, Morenc M, Ho CY, Rovito HA, *et al*. Nicotinamide Prevents UVB- and Oxidative Stress–Induced Photoaging in Human Primary Keratinocytes. The Journal of Investigative Dermatology. 2022; 142: 1670–1681.e12.

[9] Chen TH, Wang HC, Chang CJ, Lee SY. Mitochondrial Glutathione in Cellular Redox Homeostasis and Disease Manifestation. International Journal of Molecular Sciences. 2024; 25: 1314.

[10] Li J, Cao F, Yin HL, Huang ZJ, Lin ZT, Mao N, *et al*. Ferroptosis: past, present and future. Cell Death & Disease. 2020; 11: 88.

[11] Wang J, Shi J, Xiao Y, Chen G, Yang C, Duan L, *et al*. Fo-Shou-San Ameliorates Chronic Cerebral Hypoperfusion-Induced Cognitive Impairment in Mice by Regulating NRF2/HO-1 Pathway Against Ferroptosis. Journal of Integrative Neuroscience. 2023; 22: 41.

[12] Feng Z, Qin Y, Huo F, Jian Z, Li X, Geng J, *et al*. NMN recruits GSH to enhance GPX4-mediated ferroptosis defense in UV irradiation induced skin injury. Biochimica et Biophysica Acta. Molecular Basis of Disease. 2022; 1868: 166287.

[13] Vats K, Kruglov O, Mizes A, Samovich SN, Amoscato AA, Tyurin VA, *et al*. Keratinocyte death by ferroptosis initiates skin inflammation after UVB exposure. Redox Biology. 2021; 47: 102143.

[14] Ren H, Shao Y, Wu C, Ma X, Lv C, Wang Q. Metformin alleviates oxidative stress and enhances autophagy in diabetic kidney disease via AMPK/SIRT1-FoxO1 pathway. Molecular and Cellular Endocrinology. 2020; 500: 110628.

[15] Zhang Y, Liu Y, Liu X, Yuan X, Xiang M, Liu J, *et al*. Exercise and Metformin Intervention Prevents Lipotoxicity-Induced Hepatocyte Apoptosis by Alleviating Oxidative and ER Stress and Activating the AMPK/Nrf2/HO-1 Signaling Pathway in db/db Mice. Oxidative Medicine and Cellular Longevity. 2022; 2022: 2297268.

[16] Gouveri E, Papanas N. The Endless Beauty of Metformin: Does It Also Protect from Skin Aging? A Narrative Review. Advances in Therapy. 2023; 40: 1347–1356.

[17] Monte-Serrano J, Villagrasa-Boli P, Cruañes-Monferrer J, Arbués-Espinosa P, Martínez-Cisneros S, García-Gil MF. The role of metformin in the treatment of dermatological diseases: A narrative review. Atencion Primaria. 2022; 54: 102354. (In Spanish)

[18] Papaccio F, D Arino A, Caputo S, Bellei B. Focus on the Contribution of Oxidative Stress in Skin Aging. Antioxidants. 2022; 11: 1121.

[19] Zhang J, Yu H, Man MQ, Hu L. Aging in the dermis: Fibroblast senescence and its significance. Aging Cell. 2024; 23: e14054.

[20] Chin T, Lee XE, Ng PY, Lee Y, Dreesen O. The role of cellular senescence in skin aging and age-related skin pathologies. Frontiers in Physiology. 2023; 14: 1297637.

[21] Zargaran D, Zoller F, Zargaran A, Weyrich T, Mosahebi A. Facial skin ageing: Key concepts and overview of processes. International Journal of Cosmetic Science. 2022; 44: 414–420.

[22] Spierings NMK. Evidence for the Efficacy of Over-the-counter Vitamin A Cosmetic Products in the Improvement of Facial Skin Aging: A Systematic Review. The Journal of Clinical and Aesthetic Dermatology. 2021; 14: 33–40.

[23] Gaikwad SS, Zanje AL, Somwanshi JD. Advancements in transdermal drug delivery: A comprehensive review of physical penetration enhancement techniques. International Journal of Pharmaceutics. 2024; 652: 123856.

[24] Han HS, Hong JY, Kwon TR, Lee SE, Yoo KH, Choi SY, *et al*. Mechanism and clinical applications of needle-free injectors in dermatology: Literature review. Journal of Cosmetic Dermatology. 2021; 20: 3793–3801.

[25] Wang J, Chen Y, He J, Li G, Chen X, Liu H. Anti-Aging Effect of the Stromal Vascular Fraction/Adipose-Derived Stem Cells in a Mouse Model of Skin Aging Induced by UVB Irradiation. Frontiers in Surgery. 2022; 9: 950967.

[26] Mostafa DK, Nayel OA, Abdulmalek S, Abdelbary AA, Ismail CA. Modulation of autophagy, apoptosis and oxidative stress: a clue for repurposing metformin in photoaging. Inflammopharmacology. 2022; 30: 2521–2535.

[27] Berry K, Hallock K, Lam C. Photoaging and Topical Rejuvenation. Clinics in Plastic Surgery. 2023; 50: 381–390.

[28] Sadick N, Pannu S, Abidi Z, Arruda S. Topical Treatments for Photoaged Skin. Journal of Drugs in Dermatology. 2023; 22: 867–873.

[29] Duman M, Vaquié A, Nocera G, Heller M, Stumpe M, Siva Sankar D, *et al*. EEF1A1 deacetylation enables transcriptional activation of remyelination. Nature Communications. 2020; 11: 3420.

[30] Permatasari F, Hu YY, Zhang JA, Zhou BR, Luo D. Anti-photoaging potential of Botulinum Toxin Type A in UVB-

induced premature senescence of human dermal fibroblasts in vitro through decreasing senescence-related proteins. Journal of Photochemistry and Photobiology. B, Biology. 2014; 133: 115–123.

[31] Liu Y, Huang X, Wang P, Pan Y, Cao D, Liu C, *et al*. The effects of HSP27 against UVB-induced photoaging in rat skin. Biochemical and Biophysical Research Communications. 2019; 512: 435–440.

[32] Wang M, Guo Y, Wan M, Chen Z, Zhong JL. TAZ Reduces UVA-mediated Photoaging through Regulates Cell Proliferation in Skin Fibroblasts. Photochemistry and Photobiology. 2023; 99: 153–159.

[33] Chaiprasongsuk A, Panich U. Role of Phytochemicals in Skin Photoprotection *via* Regulation of Nrf2. Frontiers in Pharmacology. 2022; 13: 823881.

[34] Ikehata H, Yamamoto M. Roles of the KEAP1-NRF2 system in mammalian skin exposed to UV radiation. Toxicology and Applied Pharmacology. 2018; 360: 69–77.

[35] Yang W, Wang Y, Zhang C, Huang Y, Yu J, Shi L, *et al*. Maresin1 Protect Against Ferroptosis-Induced Liver Injury Through ROS Inhibition and Nrf2/HO-1/GPX4 Activation. Frontiers in Pharmacology. 2022; 13: 865689.

[36] Kerns ML, Chien AL, Kang S. A Role for NRF2-Signaling in the Treatment and Prevention of Solar Lentigines. Plastic and Reconstructive Surgery. 2021; 148: 27S–31S.

[37] Kerns ML, Miller RJ, Mazhar M, Byrd AS, Archer NK, Pinkser BL, *et al*. Pathogenic and therapeutic role for NRF2 signaling in ultraviolet light-induced skin pigmentation. JCI Insight. 2020; 5: e139342.

[38] Piao MJ, Fernando PMDJ, Kang KA, Fernando PDSM, Herath HMUL, Kim YR, *et al*. Rosmarinic Acid Inhibits Ultraviolet B-Mediated Oxidative Damage via the AKT/ERK-NRF2-GSH Pathway *In Vitro* and *In Vivo*. Biomolecules & Therapeutics. 2024; 32: 84–93.

[39] Baird L, Yamamoto M. The Molecular Mechanisms Regulating the KEAP1-NRF2 Pathway. Molecular and Cellular Biology. 2020; 40: e00099-20.

[40] Ma WQ, Sun XJ, Zhu Y, Liu NF. Metformin attenuates hyperlipidaemia-associated vascular calcification through anti-ferroptotic effects. Free Radical Biology & Medicine. 2021; 165: 229–242.

[41] Alnaaim SA, Al-Kuraishy HM, Al-Gareeb AI, Ali NH, Alexiou A, Papadakis M, *et al*. New insights on the potential anti-epileptic effect of metformin: Mechanistic pathway. Journal of Cellular and Molecular Medicine. 2023; 27: 3953–3965.

[42] Xu Z, Pan Z, Jin Y, Gao Z, Jiang F, Fu H, *et al*. Inhibition of PRKAA/AMPK (Ser485/491) phosphorylation by crizotinib induces cardiotoxicity via perturbing autophagosome-lysosome fusion. Autophagy. 2024; 20: 416–436.

[43] Xia Y, Zhang H, Wu X, Xu Y, Tan Q. Resveratrol activates autophagy and protects from UVA-induced photoaging in human skin fibroblasts and the skin of male mice by regulating the AMPK pathway. Biogerontology. 2024. (online ahead of print)

[44] Hegedűs C, Boros G, Fidrus E, Kis GN, Antal M, Juhász T, *et al*. PARP1 Inhibition Augments UVB-Mediated Mitochondrial Changes-Implications for UV-Induced DNA Repair and Photocarcinogenesis. Cancers. 2019; 12: 5.

[45] Zhang JA, Luan C, Huang D, Ju M, Chen K, Gu H. Induction of Autophagy by Baicalin Through the AMPK-mTOR Pathway Protects Human Skin Fibroblasts from Ultraviolet B Radiation-Induced Apoptosis. Drug Design, Development and Therapy. 2020; 14: 417–428.

[46] Zhao Y, Lin J, Li J, Bwalya C, Xu Y, Niu Y, *et al*. RhFGF21 Protects Epidermal Cells against UVB-Induced Apoptosis through Activating AMPK-Mediated Autophagy. International Journal of Molecular Sciences. 2022; 23: 12466.

[47] Wu CL, Qiang L, Han W, Ming M, Viollet B, He YY. Role of AMPK in UVB-induced DNA damage repair and growth control. Oncogene. 2013; 32: 2682–2689.

[48] Wan YS, Wang ZQ, Shao Y, Voorhees JJ, Fisher GJ. Ultraviolet irradiation activates PI 3-kinase/AKT survival pathway via EGF receptors in human skin *in vivo*. International Journal of Oncology. 2001; 18: 461–466.

[49] Hwang SY, Chae JI, Kwak AW, Lee MH, Shim JH. Alternative Options for Skin Cancer Therapy via Regulation of AKT and Related Signaling Pathways. International Journal of Molecular Sciences. 2020; 21: 6869.

[50] Kulshrestha S, Goel A. Protein therapeutics as an emerging strategy to deal with skin cancer: A short review. Experimental Dermatology. 2024; 33: e14981.

[51] Chen Q, Zhang H, Yang Y, Zhang S, Wang J, Zhang D, *et al*. Metformin Attenuates UVA-Induced Skin Photoaging by Suppressing Mitophagy and the PI3K/AKT/mTOR Pathway. International Journal of Molecular Sciences. 2022; 23: 6960.